Heat perturbation spreading in the Fermi-Pasta-Ulam-β system with next-nearest-neighbor coupling: Competition between phonon dispersion and nonlinearity

Daxing Xiong*
Department of Physics, Fuzhou University, Fuzhou, 350108 Fujian, China
(Received 25 April 2017; revised manuscript received 6 June 2017; published 30 June 2017)

We employ the heat perturbation correlation function to study thermal transport in the one-dimensional Fermi-Pasta-Ulam-β lattice with both nearest-neighbor and next-nearest-neighbor couplings. We find that such a system bears a peculiar phonon dispersion relation, and thus there exists a competition between phonon dispersion and nonlinearity that can strongly affect the heat correlation function's shape and scaling property. Specifically, for small and large anharmoncities, the scaling laws are ballistic and superdiffusive types, respectively, which are in good agreement with the recent theoretical predictions; whereas in the intermediate range of the nonlinearity, we observe an unusual multiscaling property characterized by a *nonmonotonic* delocalization process of the central peak of the heat correlation function. To understand these multiscaling laws, we also examine the momentum perturbation correlation function and find a transition process with the same turning point of the anharmonicity as that shown in the heat correlation function. This suggests coupling between the momentum transport and the heat transport, in agreement with the theoretical arguments of mode cascade theory.

DOI: 10.1103/PhysRevE.95.062140

I. INTRODUCTION

Despite decades of research, our understanding of anomalous heat transport in one-dimensional (1D) momentum-conserving systems is still scarce [1–3]. There are various theoretical models and three main numerical approaches that are devoted to solving this issue. The theoretical techniques include the mode coupling theory [4,5], the renormalization group method [6], the mode cascade assumption [7–10], the phenomenological Lévy walk model [11,12], the nonlinear fluctuating hydrodynamics theory [13,14], etc. The first two numerical approaches are based on either the direct nonequilibrium molecular dynamics simulations [15–19] or the Green-Kubo formula [20–22]. In the former, the ends of the system are first connected to heat baths with a small temperature difference for a long time. After a steady state has been obtained, one then observes the heat current flowing across the system and finally derives the thermal conductivity. In the latter, one usually examines the long time asymptotic behavior of the heat current autocorrelation function (or power spectra) and then uses the Green-Kubo formula to get the heat conductivity. In this respect, the first three theoretical models [4–10] are just devoted to the prediction of the time-scaling behavior of the heat current autocorrelation function. In particular, the mode cascade theory suggested that one should take the coupling between the momentum transport and the heat transport into account and demonstrated that, due to this coupling, to obtain an accurate prediction, the heat current power spectra at sufficiently low frequencies should be probed [7–10].

The third numerical approach is based on the perturbation correlation functions. This is inspired by the idea of diffusion of energy in the lattice systems. As is well known, in such many-body systems, particles are located mainly around their equilibrium positions. So there is no sense to talk about the diffusion of energy of the associated particles. Whereas the collective system dynamics creates a "tissue," which can react to small local perturbations affecting its dynamics. Eventually, the propagation of perturbations defines the overall information of transport [11,23–26].

With such an idea in mind, understanding the energy and heat transport processes via their perturbation correlation functions is a relevant fascinating topic of theoretical research [11–14,27–37]. The early numerical works indicated that, for general 1D nonlinear nonintegrable momentum-conserving systems, a quasisuperdiffusive Lévy walk profile of the energy perturbation correlation function can always be observed [12,27–29], which is the evidence of anomalous heat transport. Viewing this fact, such superdiffusive transport has subsequently been understood from the single particle's Lévy walk model in the superdiffusive regime after considering the particle's velocity fluctuations [11,12], although the connection between them is only phenomenological [11]. Later, a more detailed mechanism has been considered in a broad context of hydrodynamics [13,14] where the authors developed a nonlinear version of the hydrodynamics theory and explained the observed Lévy walk profile as a combination of the heat and sound modes' correlations [13,14,29]. The main achievement of this hydrodynamics theory is that it can be used to predict the scaling property of the heat and momentum perturbation spreading correlation functions in certain nonlinear systems and thus is greatly helpful for our understanding of anomalous heat transport [30]. This is because the heat and the sound modes' correlations usually are conjectured to correspond to the heat and the momentum perturbation correlation functions, respectively [29]. In particular, for generic systems of nonzero pressure, such as the Fermi-Pasta-Ulam-α-β (FPU-α-β) model with an asymmetric (odd) interparticle potential, the prediction for the sound modes' correlation is Kardar-Parisi-Zhang (KPZ) scaling [38]; whereas for the particular FPU-β system with symmetric (even) interparticle potential, it is not KPZ but Gaussian scaling [13,29]. This is consistent with the argument that the momentum current power spectrum does (does not) diverge at low frequencies for systems with odd (even) interparticle potentials [4,7–10].

Despite these achievements, an unclear point from the nonlinear hydrodynamics theory may be that we still do not

*phyxiongdx@fzu.edu.cn

know to what extent of the strength of the nonlinearity it would be applicable. Since the theory aims at dealing with the nonlinear systems, it requires the system's dynamics to be sufficiently chaotic so as to have good mixing in time [14]. So it is quite possible that, for certain linear integrable systems, the nonlinear hydrodynamics theory is not valid anymore [34]. As for the latter systems, a recent concept called "phonon random walks" might be worthwhile [39], based on which the linear system's ballistic heat perturbation spreading correlation function can instead be understood by a quantumlike wave function's modulus square where the different systems' distinct phonon dispersion relations are a key factor. In addition, in this theory the momentum perturbation correlation function is proved to be the corresponding wave function's real part [39].

Combining the above reviewing progress, one may recognize that the coupling between the heat transport and the momentum transport should naturally exist and this coupling will be exhibited quite differently in various systems. This then leads to the fact that different theoretical models would be applicable to different systems or to the same system under different strengths of the nonlinearity. In particular, for the strongly nonlinear systems where the effects of nonlinearity dominate, the nonlinear hydrodynamics theory [13,14] could present some universal predictions; whereas as for the linear systems without including the nonlinearity, the phonon dispersion relation now plays a major role [39], and there is no mode and mode's coupling [40]. Therefore, to provide a complete picture of thermal transport, such as the normal, ballistic, and superdiffusive types, and to understand the coupling between the heat transport and the momentum transport in different situations, both the effects of nonlinearity and the phonon dispersion relation are crucial and necessary to take into account. Motivated by this and in view of the fact that almost all of the above literature only focused on the systems with nearest-neighbor (NN) interaction, we here consider a 1D FPU-β system with both the NN and the next-nearest-neighbor (NNN) interactions. The advantage of this system is that it bears a peculiar phonon dispersion relation. With this advantage, we then can adjust the strength of the nonlinearity to see how such a particular phonon dispersion relation could, together with the nonlinearity, affect the system's heat transport and its scaling property. Such a research strategy also will help us to reveal the detailed coupling between the heat transport and the momentum transport in this particular system, which may provide insight into further developing a theory to bridge our present understanding of linear and nonlinear systems' thermal transport after combining both factors of the phonon dispersion relation and nonlinearity.

The rest of this paper is structured in the following way: In Sec. II we introduce the reference model and emphasize its peculiar phonon dispersion relation. Section III describes the simulation method to derive the corresponding perturbations correlation functions. In Sec. IV we present our main results, and Sec. V is devoted to a discussion of the mechanism. Finally we close with a summary in Sec. VI.

II. MODEL

As mentioned, in what follows we focus on a 1D FPU-β lattice with both NN and NNN interactions [41]. Such a system's Hamiltonian is

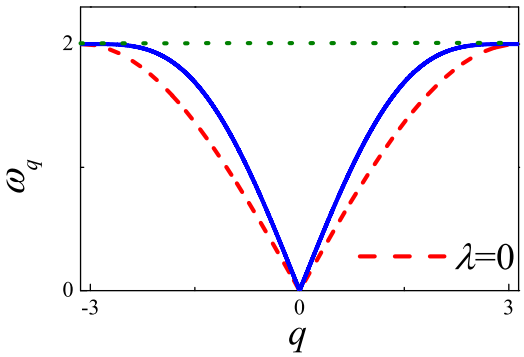

FIG. 1. The phonon dispersion relation for the FPU-β chain with both NNN and NN couplings ($\lambda = 0.25$), which is compared to the counterpart harmonic chain of $\lambda = 0$ (the dashed line). The horizontal dotted line indicates $\omega_q = 2$ near the Brillouin zone boundary.

$$H = \sum_{k=1}^{L}\left[\frac{p_k^2}{2} + V(r_{k+1} - r_k) + \lambda V(r_{k+2} - r_k)\right], \quad (1)$$

with r_k as the displacement of the kth particle from its equilibrium position and p_k as its momentum. The potential takes the FPU-β type of $V(\xi) = \xi^2/2 + \beta\xi^4/4$ with β to be adjustable and representing the nonlinearity. The parameter λ controls the comparative strength of the NNN coupling to the NN coupling, and if it is fixed at $\lambda = 0.25$ reproducing a special phonon dispersion relation (under harmonic approximation),

$$\omega_q = \sqrt{4\,\sin^2(q/2) + \sin^2(q)}, \quad (2)$$

as shown in Fig. 1. Here q is the wave number, and ω_q is the corresponding frequency. From Fig. 1 we know that such a phonon dispersion relation has a main feature, i.e., the group velocity $v_g = d\omega_q/dq$ is very close to zero in a wider q domain near the Brillouin zone boundary. This unusual property can favor the formation of a special highly localized excitation [intraband discrete breathers (DBs)] [42] in the presence of appropriate nonlinearity and thus is conjectured to greatly influence thermal transport [41]. In addition, we note that some recent works have indicated that the FPU-β lattice including such kinds of long range interactions beyond the NN couplings can lead to some unusual effects on thermal transport [43] and thermal rectification [44]. All of these understandings are also the motivations that we choose to study in such a system.

III. METHOD

We will employ the equilibrium fluctuation-correlation method [27,29] to investigate the propagation of heat perturbation. This approach has first been proposed by Zhao [27] for studying the site-site total energy fluctuations spreading and then extended to be applicable to investigate the space-space fluctuation spreading [29]. For further detailed implementation, one also can refer to Ref. [45]. Due to the apparent advantage of avoiding the emerging statistical fluctuations [11,12], such a popular efficient simulation method has widely been used in many publications [12,28,31–33,35–37].

To make a comparison with the prediction of hydrodynamics theory [13,14], we will focus on the following two space-space correlation functions of the heat perturbations and momentum perturbations [29], i.e.,

$$\rho_Q(m,t) = \frac{\langle \Delta Q_j(t) \Delta Q_i(0) \rangle}{\langle \Delta Q_i(0) \Delta Q_i(0) \rangle}, \tag{3}$$

and

$$\rho_p(m,t) = \frac{\langle \Delta p_j(t) \Delta p_i(0) \rangle}{\langle \Delta p_i(0) \Delta p_i(0) \rangle}, \tag{4}$$

respectively. Here $m = j - i$; $\langle \cdot \rangle$ denotes the spatiotemporal average. To describe the space-space correlation, one can divide the 1D lattice into several equivalent bins, and thus, i and j are the labels of the bins. In practice, we will set the averaged number of particles in each bin to be $N_i = (L-1)/b$ with b as the total number of the bins. Under such a space description, $\Delta Q_i(t) \equiv Q_i(t) - \langle Q_i \rangle$ and $\Delta p_i(t) \equiv p_i(t) - \langle p_i \rangle$ then define the heat perturbations and momentum perturbations in the ith bin at time t, respectively, with $Q_i(t)$ and $p_i(t)$ as the corresponding heat energy and momentum densities. $p_i(t)$ is easy to calculate, and one just needs to sum the related single particle's momentum $p_k(t)$ within the bin, namely, $p_i(t) \equiv \sum_k p_k(t)$. To compute $Q_i(t)$, we employ the definition of $Q_i(t) \equiv E_i(t) - \frac{(\langle E \rangle + \langle F \rangle) M_i(t)}{\langle M \rangle}$ [46,47] from thermodynamics, where $E_i(t) \equiv \sum_k E_k(t)$, $M_i(t) \equiv \sum_k M_k(t)$, and $F_i(t) \equiv \sum_k F_k(t)$ are the total energy, number of particles, and internal pressure in that bin, respectively, with $E_k(t)$, $M_k(t)$, and $F_k(t)$ as the corresponding single particle's energy, density, and pressure. From the perspective of hydrodynamics theory, $\rho_Q(m,t)$ and $\rho_p(m,t)$ might represent the heat mode's and sound modes' correlations, respectively [13,14,29], based on which one might be able to construct the corresponding energy and particle perturbation correlation functions [29]. Therefore, our following study of $\rho_Q(m,t)$ and $\rho_p(m,t)$ also is partially motivated by this connection.

The simulations of both correlation functions are performed as follows: Initially we contact the system with a Langevin heat bath [1,2] of temperature $T = 0.5$ (fixed throughout the paper) to get an equilibrium state. Then after this thermalized equilibrium state has been prepared, we utilize the Runge-Kutta integration algorithm of seventh to eighth order with a time step of $h = 0.05$ to evolve the system. During such an evolution, we then sample the relevant data and calculate the corresponding correlation functions.

To perform the simulations, we apply the following settings: periodic boundary conditions with a size of $L = 4001$–6001 is adopted, which will allow a perturbation of heat and momentum located at the center of the chain to spread out for a long time up to $t = 900$ for different β's. β is adjusted in a wide range from $\beta = 0$ (linear case) to $\beta = 1.5$ (representing the highly nonlinear case). The number of the bin is fixed at $b \equiv (L-1)/2$ and has been verified to be efficient to derive the space-space correlation information. The size of the ensemble for detecting both correlation functions is about 8×10^9.

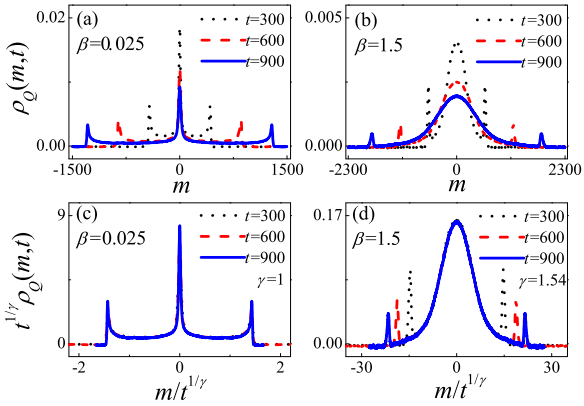

FIG. 2. (a) and (b) Profiles of $\rho_Q(m,t)$; (c) and (d) rescaled $\rho_Q(m,t)$ under formula (6). Here, three long times $t = 300$ (dotted lines), $t = 600$ (dashed lines), and $t = 900$ (solid lines) and two β values $\beta = 0.025$ and $\beta = 1.5$ are considered for comparison.

IV. RESULTS

A. Scaling for linear and highly nonlinear cases

We start with studying the following two limiting cases. The first one is the linear system with $\beta = 0$ for which one can use the formula from the theory of phonon random walks [39],

$$\rho_Q(m,t) \simeq \left| \frac{1}{2\pi} \int_{-\pi}^{\pi} e^{i(mq - \omega_q t)} dq \right|^2 \tag{5}$$

to predict $\rho_Q(m,t)$. Inserting the phonon dispersion (2) into formula (5), one then gains the prediction of $\rho_Q(m,t)$, which has been verified well by simulations [39]. The second is the highly nonlinear case. For such systems, the nonlinear hydrodynamics theory [13,14] has predicted the heat mode's correlation function to be the Lévy distribution and satisfying the following scaling property [11,12]:

$$t^{1/\gamma} \rho_Q(m,t) \simeq \rho_Q\left(\frac{m}{t^{1/\gamma}}, t \right), \tag{6}$$

with $\gamma = 3/2$ as the predicted scaling exponent. Note that such a prediction of the γ value requires the associated potential of the system to be symmetric and the internal averaged pressure $\langle F \rangle$ to be zero, and our focused system here naturally bears such a property.

With such theoretical understanding, now let us turn to the simulation results. Figure 2 presents the profiles of $\rho_Q(m,t)$ and their scaling properties for three typical times and two β values, among which, $\beta = 0.025$ denotes the system close to the linear case; whereas $\beta = 1.5$ we employ to represent the highly nonlinear case. As expected, on one hand, at the relatively small β value, the profile of $\rho_Q(m,t)$ is mainly dependent on the phonon dispersion relation (2) determined by formula (5) and following the ballistic scaling ($\gamma = 1$) [see Figs. 2(a) and 2(c)] if compared to the prediction of Ref. [39], especially, we can see a highly localized peak on the origin ($m = 0$). Such a localized peak of $\rho_Q(m,t)$ mainly stems from the special phonon dispersion relation [Eq. (2) and Fig. 1] where as we already have mentioned that there is a wider q domain with zero group velocities near the Brillouin zone boundary. On the other hand, the situation for

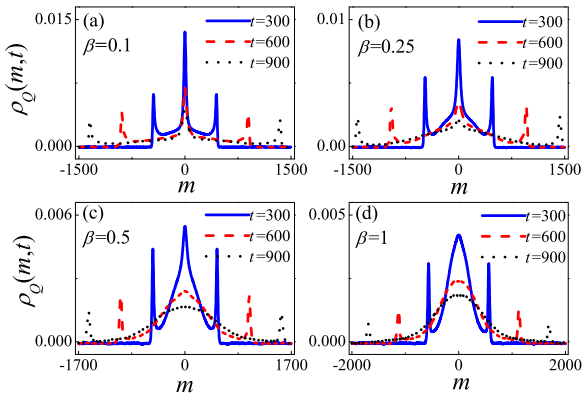

FIG. 3. Profiles of $\rho_Q(m,t)$ for three long times $t = 300$ (solid lines), $t = 600$ (dashed lines), and $t = 900$ (dotted lines) and four β values in the intermediate range: (a) $\beta = 0.1$, (b) $\beta = 0.25$, (c) $\beta = 0.5$, and (d) $\beta = 1$.

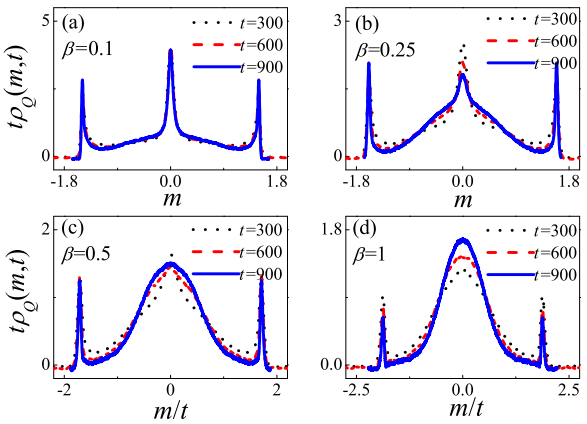

FIG. 4. Rescaled $\rho_Q(m,t)$ according to formula (6) with $\gamma = 1$ for three long times $t = 300$ (dotted lines), $t = 600$ (dashed lines), and $t = 900$ (solid lines) and four β values in the intermediate range: (a) $\beta = 0.1$, (b) $\beta = 0.25$, (c) $\beta = 0.5$, and (d) $\beta = 1$.

the cases of relatively large nonlinearity is quite different: The highly localized central peak now disappears, instead, a common quasisuperdiffusive ($\gamma = 1.54$) Lévy walk profile can be observed [see Figs. 2(b) and 2(d)]. This seems to indicate that the nonlinearity can cause the delocalization of $\rho_Q(m,t)$ in a certain domain induced by the phonon dispersion relation. Therefore, it would be interesting to study in more detail such a delocalization process, which may help us to fully understand both roles of phonon dispersion and nonlinearity.

B. Multiscaling in the intermediate range of nonlinearity

Before going on, let us first see some typical profiles of $\rho_Q(m,t)$ in the intermediate range of β values to gain a preliminary impression. Figure 3 presents such a result from which a detailed crossover from localization to delocalization of the central peak of $\rho_Q(m,t)$ can clearly be identified. Since such an unusual localized shape is exhibited in the center, one can expect that the scaling formula (6) is now no longer valid, but whatever one can first use that scaling formula with $\gamma = 1$ to rescale the profiles to see how the ballistic transport (mainly induced by the phonon dispersion dispersion) can be destroyed by increasing the nonlinearity. For such a purpose, in Fig. 4 we plot the result of rescaled $\rho_Q(m,t)$ under ballistic scaling ($\gamma = 1$). As can be seen, with the increase in β, indeed, the distortion of ballistic scaling first originates from the central part and then walks towards the direction of the front parts, whereas it should be noted that, if one only looks at the front peaks, the ballistic scaling still seems available. Viewing this fact, it is reasonable to conjecture that $\rho_Q(m,t)$ should at least bear two-scaling behaviors: $\gamma = 1$ for the front peaks and $\gamma \neq 1$ for the others. To further verify this multiscaling property, we here follow Refs. [48–50] to study the s ($s > 0$) order momentum of $\rho_Q(m,t)$, i.e., $\langle |m(t)|^s \rangle = \int_{-\infty}^{\infty} |m(t)|^s \rho_Q(m,t) dm$ from which for the strong anomalous diffusion process $\langle |m(t)|^s \rangle$ has been conjectured to follow $\langle |m(t)|^s \rangle \sim t^{s\nu(s)}$ with $\nu(s)$ as a s-dependent exponent [50]; whereas for the ballistic (normal) transport, it is easy to find that $\nu(s)$ will be close to 1 (1/2). Therefore, this s-dependent scaling exponent $s\nu(s)$ is useful to characterize anomalous superdiffusive thermal transport, distinct from both ballistic and normal cases.

Figure 5 depicts the results of $s\nu(s)$ versus s calculated from $\rho_Q(m,t)$ for several typical β values from small to large. As can be seen, with the increase in β, $s\nu(s)$ first shows a single linear scaling with s [see Fig. 5(a)], indicating $\nu(s) \approx 1$ and suggesting the ballistic heat transport; then at about $\beta = 0.1$ this single-scaling behavior is destroyed for low order s, eventually, a bilinear scaling behavior starts to appear [see Fig. 5(b)]; finally, for the relatively large β values, we see a scaling exponent for the low order s, denoted by $\nu^L(s)$, close to $\nu^L(s) \approx 0.6$ to 0.7 [see Fig. 5(f)].

It would be worthwhile to note that such a particular bilinear scaling behavior has recently been addressed theoretically in the Lévy walk model within the superdiffusive regime [its density follows the scaling formula (6) with $1 < \gamma < 2$], where γ is explained as the power-law exponent from the waiting time distribution $\phi(\tau) \sim \tau^{-1-\gamma}$ of the model (see Refs. [48,49] for details). In the Lévy walk model, $\nu^L(s)$ is predicted to be $1/\gamma$ [48,49]. Therefore, essentially $\nu^L(s)$ involves important

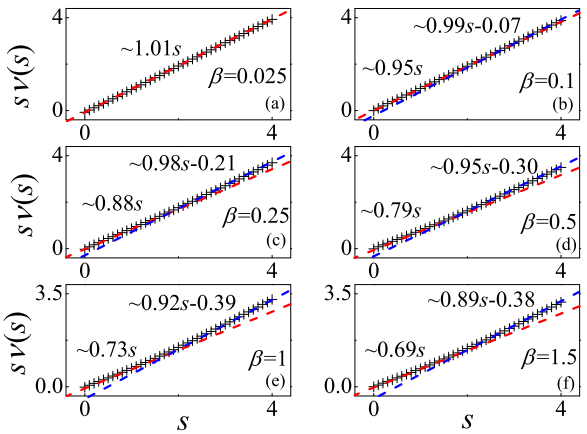

FIG. 5. $s\nu(s)$ versus s for indicating the multiscaling property of $\rho_Q(m,t)$ for (a) $\beta = 0.025$, (b) $\beta = 0.1$, (c) $\beta = 0.25$, (d) $\beta = 0.5$, (e) $\beta = 1$, and (f) $\beta = 1.5$, respectively.

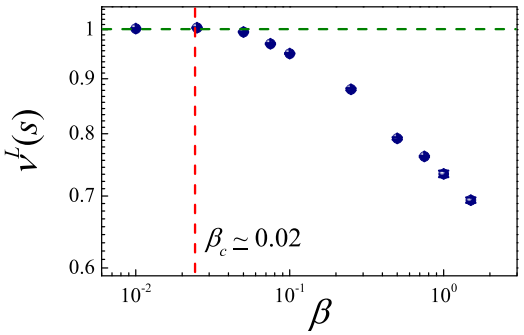

FIG. 6. The fitting values of $\nu^L(s)$ versus β where the horizontal (vertical) dashed line represents $\nu(s) = 1$ ($\beta_c \simeq 0.02$).

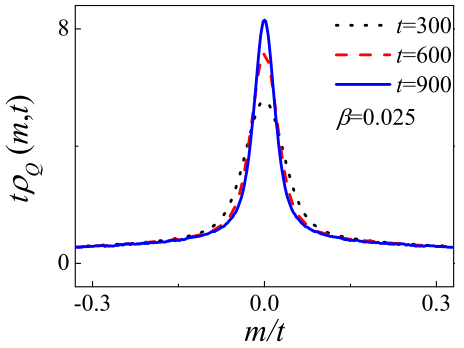

FIG. 7. Rescaled $\rho_Q(m,t)$ under the ballistic scaling ($\gamma = 1$) for $\beta = 0.025$ to indicate that, for the central peak, the ballistic scaling is not perfectly valid.

information for describing superdiffusive transport. For this reason, we further examine the result of $\nu^L(s)$ versus β in Fig. 6. As can be seen, a detailed crossover from ballistic [$\nu^L(s) = 1$, thus $\gamma = 1$] to superdiffusive [$1/2 < \nu^L(s) < 1$, thus $1 < \gamma < 2$] transport at a critical point of $\beta_c \simeq 0.02$ can clearly be identified. This critical point of β_c is consistent with the same value of β_c found in the FPU-β system with NN coupling only [35] where it has been conjectured to be related to the strong stochasticity threshold of the system [51].

For the highly nonlinear case ($\beta = 1.5$, for example), bearing in mind both predictions of $\nu^L(s) = 1/\gamma$ from the Lévy walk model [48,49] and $\gamma = 3/2$ from the nonlinear hydrodynamics theory [13,14], now we make a comparison of our data with the predictions. From Fig. 5(f) we know $\nu^L(s) = 0.69$, hence γ is about 1.45 according to Refs. [48,49]. In view of the measurement errors, this result is consistent with the prediction of $\gamma = 3/2$ [13,14] and the result of $\gamma = 1.54$ from the scaling analysis as shown in Fig. 2(d).

C. Delocalization of the central peak

After studying the whole scaling property of $\rho_Q(m,t)$, let us consider the delocalization process of the central peak. In fact, since a peculiar phonon dispersion relation is exhibited in the domain near the Brillouin zone boundary (see Fig. 1), it can be expected that the scaling behavior of this central peak is more complicated. Based on this fact, the competition between phonon dispersion and nonlinearity can be revealed in more detail. To further demonstrate this point, we first employ the result of Fig. 2(c) once again, i.e., the rescaled $\rho_Q(m,t)$ under $\beta = 0.025$ to give more emphasis on the central peak's scaling. As shown in Fig. 7, clearly, although the whole shapes of $\rho_Q(m,t)$ for different t's can be nearly perfectly rescaled by ballistic scaling ($\gamma = 1$) [see Fig. 2(c)], the scaling of just this central peak shows some deviations.

Viewing this fact, next we investigate how the decay of this central peak would depend on the nonlinearity. Generally, we find that $\rho_Q(0,t)$ decays with t in a power law, i.e., $\rho_Q(0,t) \sim t^{-\eta}$ with η as a time-scaling exponent. Such relevant results for several typical β values are plotted in Fig. 8 among which we note that the result of $\beta = 0$ is derived from the theoretical formula of Eq. (5) suggesting the fact of $\eta = 1/2$ [see Fig. 8(a)]. Interestingly, compared to the whole scaling property of $\rho_Q(m,t)$, Fig. 8 indicates that the picture of the decay of $\rho_Q(0,t)$ for different t's is richer, i.e., with the increase in β, $\rho_Q(0,t)$ first decays with one single η value [see Figs. 8(a) and 8(b)]; then at about $\beta = 0.05$, an additional η value in the range of long t emerges [see Fig. 8(c)]; after that, if one increases β further, a total of three η values can be observed [see Fig. 8(d)]; whereas eventually, for the highly nonlinear case, the third scaling exponent in a long time, denoted by η^L, seems to dominate [see Fig. 8(f)]. A careful examination of the turning point from one- to two-scaling exponents suggests a critical point of $\beta_c \simeq 0.02$, which is similar to that demonstrated in Fig. 6. This implies that the time-scaling exponent η of the central peak of $\rho_Q(m,t)$ also involves key information for characterizing anomalous thermal transport.

Finally, as one usually is concerned with the long time asymptotic behavior of the heat transport property, in Fig. 9 we further plot the result of η^L versus β. One can see that, as β increases from 0.025 to 1.5, η^L increases first, then reaches its maximum value at about $\beta_{tr} \simeq 0.25$, and finally decreases down to $\eta^L \approx 3/2$ with the similar value of the scaling exponent γ shown in Fig. 2(d). Obviously, such an asymptotic decay behavior of the central peak with β is *nonmonotonic*, which is consistent with the same nonmonotonic variation of the size-dependent scaling exponent of the heat conductivity with

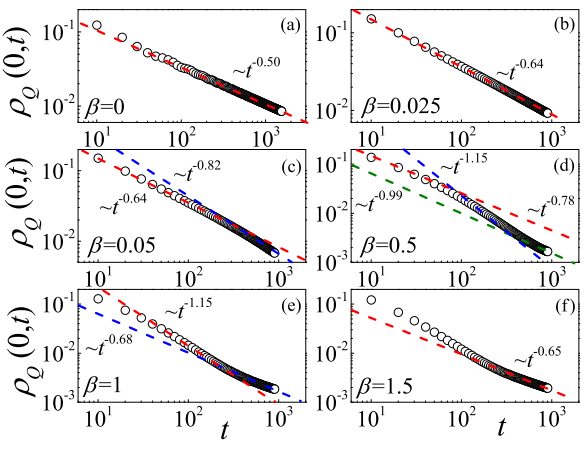

FIG. 8. $\rho_Q(0,t)$ versus t for indicating the scaling property of the central peak: (a) $\beta = 0$, (b) $\beta = 0.025$, (c) $\beta = 0.05$, (d) $\beta = 0.5$, (e) $\beta = 1$, and (f) $\beta = 1.5$, respectively.

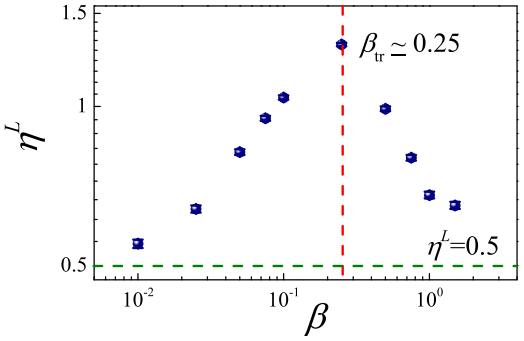

FIG. 9. η^L versus β where the horizontal (vertical) dashed line denotes $\eta^L = 0.5$ ($\beta_{tr} \simeq 0.25$).

temperature in the same model [41], thus further supporting the fact that the heat conduction of this system is nonuniveral, dependent on certain system's parameters [41].

V. DISCUSSION

We are particularly interested in the underlying mechanism of the observed nonmonotonic delocalization process of $\rho_Q(m,t)$. From the microscopic point of view, this can be understood by the property of intraband DBs [41], which is nonmonotonically dependent on the temperature, hence it is nonmonotonically dependent on the nonlinearity. Eventually if the heat transport can be understood by the picture of phonons scattered by such intraband DBs, a nonmonotonic delocalization of $\rho_Q(m,t)$ with β could be expected [41]. We here aim to explore this scattering process of phonons from a macroscopic point of view. Keeping this in mind, in the following we will employ the correlation function of momentum perturbations to reveal the information of such a scattering process.

The momentum spread described by its perturbation correlation function $\rho_p(m,t)$ contains useful information for understanding the heat transport of momentum-conserving systems. As mentioned in Sec. III, $\rho_p(m,t)$ may correspond to the sound modes' correlation in hydrodynamics theory [13,14,29]. A diffusive momentum spread has been conjectured to be the origin of the normal heat transport observed in coupled rotator systems [52]. This nonballisitic spread of momentum has also been revealed in another special system with a double-well interparticle potential [36]. In the phonon random walk theory, the momentum correlation function in linear systems has been proved to be a quantumlike wave function's real part, whereas this quantum wave function's modulus square can represent the heat perturbation correlation function [39]. A more recent work [53] developed an effective linear stochastic structure theory to derive the momentum spreading correlation function in the long time limit and demonstrated that anomalous thermal transport is dominated by the long wavelength renormalized waves [54–56].

We begin with presenting some typical results of $\rho_p(m,t)$ in Fig. 10. Here, three long times and four β values, the same as those in Fig. 3, are considered. As can be seen, all the profiles of $\rho_p(m,t)$ suggest nondiffusive ballistic behaviors, which are the evidence of anomalous heat transport. In particular, three points can be revealed: First, the moving velocities of the front

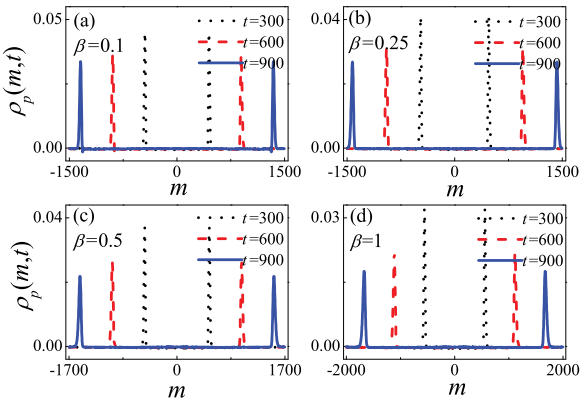

FIG. 10. Profiles of $\rho_p(m,t)$ for three long times $t = 300$ (dotted lines), $t = 600$ (dashed lines), and $t = 900$ (solid lines) and four β values in the intermediate range: (a) $\beta = 0.1$, (b) $\beta = 0.25$, (c) $\beta = 0.5$, and (d) $\beta = 1$.

peaks are increased with the increase in β, which is a natural property of the systems with hard-type anharmonicity [37], and can be understood from the renormalized wave theory [54–56]. Second, as β increases, a slight broadening of the side peaks can be identified. This broadening is related to the sound attenuation [29]. In the hydrodynamic theory [4,5,7–10,13,14], it has usually been suggested that there is a mode-dependent damping coefficient $\Gamma_q \sim D|q|^\delta$ in the small wave-number's limit, where D is a damping constant and δ is a scaling exponent. Then, the constant D can be inferred from this broadening [53].

Finally, for each β value, the front peaks of $\rho_p(m,t)$ decay with t in a power law: $h \sim t^{-\delta}$, and here h is the height of the peaks. This power-law exponent δ has been conjectured to correspond to the exponent shown in Γ_q [53]. It also may correspond to both the scaling exponents of the sound modes' correlation function predicted by the nonlinear hydrodynamics theory [13,14] and of the heat current power spectra suggested by the mode coupling [4,5] or mode cascade [7–10] theory. For this reason, we here examine, in detail, the decay of this ballistic front peak of $\rho_p(m,t)$ in some intermediate ranges of β values (see Fig. 11). Remarkably, we find that this decay behavior also shows a sensitive dependence of β. In particular,

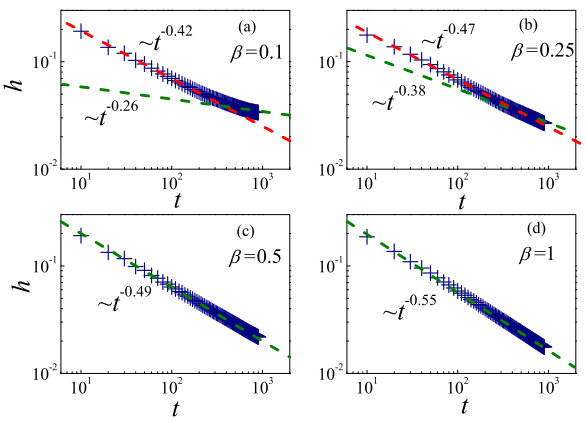

FIG. 11. The height h of the front peaks of $\rho_p(m,t)$ decays with t: (a) $\beta = 0.1$, (b) $\beta = 0.25$, (c) $\beta = 0.5$, and (d) $\beta = 1$.

around a turning point of $\beta_{\rm tr} \simeq 0.25$, there is a crossover from two-scaling exponents (for small β) to a one-scaling exponent (for large β). Eventually, for the relatively large β values, the values of δ seem to converge to a value of 0.5 to 0.6 [see Figs. 11(c) and 11(d)], which is almost consistent with the value of $\delta = 1/2$ predicted by the relevant theories in the long time limit [4,5,7–10,13,14]. However, for the relatively small β values in this intermediate range, obviously, it seems to show some deviations.

Given the same turning point of $\beta_{\rm tr} = 0.25$, it is reasonable to conjecture that there should be a close relationship between the delocalization of the central peak of $\rho_Q(m,t)$ and the decay of the side peaks of $\rho_p(m,t)$. Such a relation revealed here is amazing since the central peak of $\rho_Q(m,t)$ is contributed by phonons with high wave numbers, whereas the side peaks of $\rho_p(m,t)$ are represented by those with low q in view of their different group velocities. So, even though there are some couplings between $\rho_Q(m,t)$ and $\rho_p(m,t)$, such couplings should naturally arise at the same locations with the same q (the same group velocities) [34]. However, our results here seem to violate this natural intuition.

Turning back to the related theoretical models, the nonlinear hydrodynamics theory [13,14] claimed that, for sound modes, the correction from the coupling of the heat mode will vanish in the long time limit, but it decays very slowly, so at the intermediate time scales, one could see some physically interesting information of the heat and the sound modes' coupling. But obviously, the nonlinear hydrodynamics theory did not tell us that the coupling between the sound and the heat modes' correlation can be so unusual. As to this point, we note that the assumption of the mode cascade theory [7–10] may present a correct picture. The central argument the authors suggested is that the thermal conductivity at any (sufficiently low) frequency can be determined entirely by the thermal conductivity and bulk viscosity (represented by the momentum transport) at much higher frequencies. This sort of unusual coupling between the heat transport and the momentum transport, which is the explicit basis of the mode cascade theory [7–10], seems to be supported by our present results here, although the argument is still difficult to examine in more detail.

VI. CONCLUSION

To summarize: We have employed the heat perturbation correlation function $\rho_Q(m,t)$ to investigate anomalous thermal transport in a 1D FPU-β lattice including both the NN and the NNN interactions. After choosing an appropriate coupling ratio, we have obtained a peculiar phonon dispersion relation which then enables us to examine both roles of phonon dispersion and nonlinearity in more detail. It has been found that, for relatively small and large nonlinearities, the transports are ballistic and Lévy walk types, respectively, which can be well understood from the predictions of the concept of phonon random walks [39] and the theory of nonlinear fluctuating hydrodynamics [13,14]. Whereas more interesting things take place in the intermediate range of the nonlinearity where we emphasize that there, both the phonon dispersion relation and the nonlinearity can play roles. In this intermediate range, we have found that: (i) there is a transition from the single scaling to multiscaling for the whole profiles of $\rho_Q(m,t)$ with a critical point of $\beta_c \simeq 0.02$; (ii) the delocalization of the central peak of $\rho_Q(m,t)$ shows a *nonmonotonic* dependence of nonlinearity with another turning point of $\beta_{\rm tr} \simeq 0.25$.

The first critical point of $\beta_c \simeq 0.02$ indicates a crossover from ballistic to nonballistic transport and might be related to the strong stochasticity threshold of the focused FPU-β systems, either or not yet including the NNN interactions [35]. The second turning point of $\beta_{\rm tr} \simeq 0.25$ is a special feature of such systems and seems to be related to the nonuniversal heat conduction observed previously in the same system [41]. In those previous publications [41], we have conjectured that the microscopic underlying mechanism is caused by the scattering of phonons by intraband DBs. Here instead, we use the momentum perturbation correlation function $\rho_p(m,t)$ to explore this phonon's scattering process from a macroscopic point of view, which makes this conjecture more convincing. Remarkably, we find that the time decay behavior of the side peaks of $\rho_p(m,t)$ follows a similar nonmonotonic β-dependent manner as those shown in $\rho_Q(m,t)$.

Finally, we would like to point out that such a coincidence of the properties of $\rho_Q(m,t)$ and $\rho_p(m,t)$ suggests the very slowly decoupling process of the heat and the sound modes' correlations claimed by the nonlinear hydrodynamics theory [13,14], in particular, for the cases in the intermediate range of the nonlinearity (or at the intermediate time scales). It also supports the assumption of the mode cascade theory proposed by Lee-Dadswell *et al.* [7,8] and Lee-Daswell [9,10], i.e., the unusual coupling between the heat transport and the momentum transport should be taken into account. This is because the heat mode and the sound modes naturally are considered as contributed by the relatively high and low wave-number phonon modes with the relatively high and low frequencies, respectively.

In short, the results presented here might provide further useful information for our understanding of anomalous heat transport and its coupling to the momentum transport, particularly from the perspective of the phonon dispersion relation and nonlinearity, although understanding the detailed underlying mechanism still requires effort.

ACKNOWLEDGMENTS

This work was supported by the National Natural Science Foundation of China (Grant No. 11575046); the Natural Science Foundation of Fujian Province, China (Grant No. 2017J06002); the Training Plan Fund for Distinguished Young Researchers from the Department of Education, Fujian Province, China, and the Qishan Scholar Research Fund of Fuzhou University, China.

[1] S. Lepri, R. Livi, and A. Politi, Phys. Rep. **377**, 1 (2003).

[2] A. Dhar, Adv. Phys. **57**, 457 (2008).

[3] S. Lepri, R. Livi, and A. Politi, *Thermal Transport in Low Dimensions*, Lecture Notes in Physics Vol. 921 (Springer, Berlin, 2016).

[4] L. Delfini, S. Lepri, R. Livi, and A. Politi, Phys. Rev. E **73**, 060201 (2006).

[5] L. Delfini, S. Lepri, R. Livi, and A. Politi, J. Stat. Mech.: Theory Exp. (2007) P02007.

[6] O. Narayan and S. Ramaswamy, Phys. Rev. Lett. **89**, 200601 (2002).

[7] G. R. Lee-Dadswell, B. G. Nickel, and C. G. Gray, Phys. Rev. E **72**, 031202 (2005).

[8] G. R. Lee-Dadswell, B. G. Nickel, and C. G. Gray, J. Stat. Phys. **132**, 1 (2008).

[9] G. R. Lee-Dadswell, Phys. Rev. E **91**, 032102 (2015).

[10] G. R. Lee-Dadswell, Phys. Rev. E **91**, 012138 (2015).

[11] V. Zaburdaev, S. Denisov, and J. Klafter, Rev. Mod. Phys. **87**, 483 (2015).

[12] V. Zaburdaev, S. Denisov, and P. Hänggi, Phys. Rev. Lett. **106**, 180601 (2011).

[13] C. B. Mendl and H. Spohn, Phys. Rev. Lett. **111**, 230601 (2013).

[14] H. Spohn, J. Stat. Phys. **154**, 1191 (2014).

[15] S. Lepri, R. Livi, and A. Politi, Phys. Rev. Lett. **78**, 1896 (1997).

[16] A. Dhar, Phys. Rev. Lett. **88**, 249401 (2002).

[17] P. Grassberger, W. Nadler, and L. Yang, Phys. Rev. Lett. **89**, 180601 (2002).

[18] G. Casati and T. Prosen, Phys. Rev. E **67**, 015203 (2003).

[19] T. Mai, A. Dhar, and O. Narayan, Phys. Rev. Lett. **98**, 184301 (2007).

[20] R. Kubo, M. Toda, and N. Hashitsume, *Statistical Physics II: Nonequilirium Statistical Mechanics* (Springer, New York, 1991).

[21] D. Andrieux and P. Gaspard, J. Stat. Mech.: Theory Exp. (2007) P02006.

[22] S. Chen, Y. Zhang, J. Wang, and H. Zhao, Phys. Rev. E **89**, 022111 (2014).

[23] E. Helfand, Phys. Rev. **119**, 1 (1960).

[24] A. Torcini, P. Grassberger, and A. Politi, J. Phys. A **28**, 4533 (1995).

[25] G. Giacomelli, R. Hegger, A. Politi, and M. Vassalli, Phys. Rev. Lett. **85**, 3616 (2000).

[26] C. Primo, I. G. Szendro, M. A. Rodriguez, and J. M. Gutiérrez, Phys. Rev. Lett. **98**, 108501 (2007).

[27] H. Zhao, Phys. Rev. Lett. **96**, 140602 (2006).

[28] N. Li, B. Li, and S. Flach, Phys. Rev. Lett. **105**, 054102 (2010).

[29] S. Chen, Y. Zhang, J. Wang, and H. Zhao, Phys. Rev. E **87**, 032153 (2013).

[30] S. G. Das, A. Dhar, K. Saito, C. B. Mendl, and H. Spohn, Phys. Rev. E **90**, 012124 (2014).

[31] S. Liu, P. Hänggi, N. Li, J. Ren, and B. Li, Phys. Rev. Lett. **112**, 040601 (2014).

[32] J. Wang, D. He, Y. Zhang, J. Wang, and H. Zhao, Phys. Rev. E **92**, 032138 (2015).

[33] J. Wang, Y. Zhang, and H. Zhao, Phys. Rev. E **93**, 032144 (2016).

[34] A. Kundu and A. Dhar, Phys. Rev. E **94**, 062130 (2016).

[35] D. Xiong, Europhys. Lett. **113**, 14002 (2016).

[36] D. Xiong, J. Stat. Mech.: Theor. Exp. (2016) 043208.

[37] D. Xiong, Phys. Rev. E **95**, 042127 (2017).

[38] M. Kardar, G. Parisi, and Y. C. Zhang, Phys. Rev. Lett. **56**, 889 (1986).

[39] D. Xiong and E. Barkai, arXiv:1606.04602.

[40] Z. Rieder, J. L. Lebowitz, and E. Lieb, J. Math. Phys. **8**, 1073 (1967).

[41] D. Xiong, J. Wang, Y. Zhang, and H. Zhao, Phys. Rev. E **85**, 020102 (2012); D. Xiong, Y. Zhang, and H. Zhao, *ibid.* **90**, 022117 (2014).

[42] S. V. Dmitriev, A. P. Chetverikov, and M. G. Velarde, Phys. Status. Solidi B **252**, 1682 (2015).

[43] D. Bagchi, Phys. Rev. E **95**, 032102 (2017).

[44] M. Romero-Bastida, J. O. Miranda-Peña, and J. M. López, Phys. Rev. E **95**, 032146 (2017).

[45] P. Hwang and H. Zhao, arXiv:1106.2866.

[46] D. Forster, *Hydrodynamic Fluctuations, Broken Symmetry, and Correlation Functions* (Benjamin, New York, 1975).

[47] J. P. Hansen and I. R. McDonald, *Theory of Simple Liquids*, 3rd ed. (Academic, London, 2006).

[48] A. Rebenshtok, S. Denisov, P. Hänggi, and E. Barkai, Phys. Rev. Lett. **112**, 110601 (2014).

[49] A. Rebenshtok, S. Denisov, P. Hänggi, and E. Barkai, Phys. Rev. E **90**, 062135 (2014).

[50] P. Castiglione, A. Mazzino, P. Muratore-Ginanneschi, and A. Vulpiani, Physica D (Amsterdam) **134**, 75 (1999).

[51] S. Lepri, R. Livi, and A. Politi, in *Anomalous Transport: Foundations and Applications*, edited by R. Klages, G. Radons, and I. M. Sokolov (Wiley-VCH, Weinheim, 2008).

[52] Y. Li, S. Liu, N. Li, P. Hänggi, and B. Li, New J. Phys. **17**, 043064 (2015).

[53] S.-X. W. Jiang, H.-H. Lu, D. Zhou, and D. Cai, New J. Phys. **18**, 083028 (2016).

[54] B. Gershgorin, Y. V. Lvov, and D. Cai, Phys. Rev. Lett. **95**, 264302 (2005).

[55] B. Gershgorin, Y. V. Lvov, and D. Cai, Phys. Rev. E **75**, 046603 (2007).

[56] S.-X. W. Jiang, H.-H. Lu, D. Zhou, and D. Cai, Phys. Rev. E **90**, 032925 (2014).